Available online at www.CivileJournal.org

Civil Engineering Journal

(E-ISSN: 2476-3055; ISSN: 2676-6957)

Vol. 10, No. 01, January, 2024

Behavior of Fire-damaged RC Beams After Strengthening with Various Techniques

Asser Elsheikh [1, 2*], Hadeal H. Alzamili [1]

[1] Department of Civil Engineering, Peoples' Friendship University of Russia (RUDN), Moscow, Russian Federation.

[2] Structural Engineering Department, Mansoura University, Mansoura, Egypt.

Received 14 September 2023; Revised 15 December 2023; Accepted 20 December 2023; Published 01 January 2024

Abstract

High temperatures during a fire can significantly degrade the structural capacity of concrete. However, in many cases, it is possible to restore and strengthen fire-damaged concrete rather than completely rebuild damaged structures. The study considered two types of concrete (normal 25 MPa and high-strength 65 MPa) with two types of strengthening techniques: carbon-fiber-reinforced polymers (CFRP) sheets with different thicknesses of 1.5 and 2.5 mm and slurry-infiltrated fibrous concrete (SIFCON) jacketing with different fiber sizes of 20 and 30 mm. The numerical simulations and analyses were conducted to capture the complex behavior of fire-damaged concrete members (beams). A fire-damaged concrete beam subjected to an extreme or critical fire Exposure time (2 hours) was evaluated and modified using a finite element simulation approach. The simulation process included three stages: the first, subjecting the concrete beam to thermal loading; the second, reflecting the fire distribution map to another model of applying mechanical loading; and the third, involving the application of strengthening to the damaged model. The results showed that the strengthening using CFRP with a thickness of 2.5 improved the load-carrying capacity compared with SIFCON in both types of concrete. 200% improvement for the normal-strength concrete beam and a 136% improvement for the high-strength concrete beam, compared to the damaged beams.

Keywords: RC Beam; CFRP; SIFCON; Fire.

1. Introduction

After a fire, it is important to conduct a thorough assessment of the damaged structural organs to determine the extent of the damage. Such an assessment may include visual inspections, non-destructive tests, and material sampling to assess the residual strength and integrity of structural elements. In most cases, repair versus replacement is an optimal option, as the decision on the repair or replacement of the affected structural members is made depending on the severity of the damage. In less severe cases, such repair methods as patching, strengthening with the use of additional materials, or applying protective coatings may be sufficient. However, if the damage is extensive, a complete replacement of the damaged organ may be necessary [1].

High temperatures can cause profound changes in the properties of concrete, leading to a potential loss of strength, stiffness, and durability. Understanding the post-fire behavior of concrete is essential for evaluating the residual structural capacity and implementing effective repair and strengthening strategies. The behavior of steel reinforcement in a fire depends on several factors, including the temperature reached, the duration of exposure, and the size and condition of the concrete element, which can lead to deformation, loss of bond with the surrounding concrete, and even

* Corresponding author: assermfee@mans.edu.eg

http://dx.doi.org/10.28991/CEJ-2024-010-01-012

complete failure. The weakened or damaged reinforcement can result in a loss of structural integrity and increase the risk of collapse [2].

Fire exposure to concrete structures can lead to significant residual capacity loss, affecting future re-use. To evaluate the residual capacity of fire-damaged concrete members, an experimental approach was conducted at three stages: pre-fire exposure, during fire exposure, and post-fire exposure [3]. Results showed that the fire-damaged concrete beams retained residual capacity even after prolonged heating. The decay rate of fire exposure impacted post-fire residual capacity retention. Increased load levels and large post-fire deflections negatively impacted the serviceability limit state.

Concrete's fire resistance varies by type. High-performance concrete (HPC), characterized by advanced mix design and high-quality constituent materials, can deliver superior strength, durability, and resistance to various environmental and mechanical stresses. HPC demonstrated unique behaviors compared to normal concrete when subjected to high temperatures [1, 4]. Its denser microstructure, reduced permeability, and improved thermal stability contributed to its enhanced performance under fire conditions. Normal concrete, on the other hand, has a more typical composition and may exhibit different behaviors when exposed to high temperatures. It is generally more susceptible to thermal cracking, spalling, and overall degradation compared to HPC [1, 4]. Investigating various repair and rehabilitation techniques for fire-damaged RC structures, such as external bonding of fiber-reinforced polymers (FRP), concrete jacketing, and steel plate bonding, can help identify the most effective methods for restoring the structural performance and durability of damaged members. By addressing these and other aspects of repairing fire-damaged RC structures, it can contribute to the development of robust and reliable repair strategies that enhance the safety, resilience, and longevity of reinforced concrete construction in the face of fire-related challenges.

Using carbon fiber-reinforced polymer (CFRP) sheets to enhance the behavior of fire-damaged concrete elements is an innovative approach in the field of structural rehabilitation and repair. The application of CFRP sheets offers a viable solution for restoring the structural integrity and load-carrying capacity of fire-damaged concrete members, including beams, columns, and slabs. By providing external confinement and strengthening, CFRP sheets can effectively mitigate the detrimental effects of fire-induced damage and contribute to the overall resilience of the structure.

Elevated temperatures, especially beyond 500°C, could have severe detrimental effects on concrete structures [2]. These effects are primarily caused by the vapor pressure, decomposition of cement hydration products, and inhomogeneous volume changes of concrete's ingredients. When concrete is exposed to high temperatures, the water trapped within the concrete pores begins to vaporize [2]. As the water vaporizes, pressure is created within the concrete. This increase in vapor pressure causes the spalling of concrete, where surface layers of the concrete break off due to the rapid expansion of the water vapor.

The ability of CFRP to recover shear strength, ductility, bending, and load capacity has been investigated by Zhou and Wang [5]. The results approved the efficiency of using CFRP sheets in enhancing the behavior of fire-damaged concrete elements. A new type of CFRP called pre-saturated CFRP (PS-CFRP) has been introduced by Naqvi [6]. PS-CFRP was pre-impregnated with epoxy resin, which enhanced its bonding capability and improved its performance. The results of using PS-CFRP for strengthening beams and columns in reinforced concrete structures showed improvements compared to regular CFRP. The behavior of ultra-high-performance fiber-reinforced concrete (UHPFC) deep beams was investigated, focusing on their strength and resistance to elevated temperatures [7]. An analytical model was developed to predict the load-carrying capacity of UHPFC deep beams strengthened after exposure to elevated temperatures. The beams were tested at ambient and 450 °C temperatures, with CFRP sheets and CFRP U-wrap strips used for strengthening. Results showed a significant impact on post-peak behavior and excellent performance in improving post-cracking behavior, shear strength, energy-based ductility index, and deflection ductility index.

Integrating CFRP sheets as internal reinforcement within the maximum bending zone of thermally damaged beams has been proposed by Al-Rousan [8]. Experimental tests have shown that this internal strengthening approach outperforms traditional external reinforcement methods. This internal CFRP reinforcement significantly enhanced the mechanical characteristics and overall behavior of RC beams, providing a promising strategy for improving their performance and durability.

The bond behavior of cement-based adhesives and CFRP strips with innovative surface treatments has been studied by Mohammadi-Firouz et al. [9]. The CFRP strips were manufactured with sand-treated surfaces to improve bonding performance. Pull-out tests showed that applying sand treatment to the CFRP strips increased the maximum pull-out force up to 12 times. The average bond strength was 9 MPa and 11 MPa, respectively, with the proposed strengthening system able to withstand up to 30 minutes of heat exposure before bond failure.

On the other hand, the use of Slurry-Infiltrated Fibrous Concrete (SIFCON) as a strengthening material after fire damage represents an innovative and promising approach in the field of structural rehabilitation and repair. In the aftermath of a fire event, concrete elements often suffer from a significant reduction in strength and durability, necessitating effective restoration and strengthening techniques [10, 11].

SIFCON offers a viable solution for enhancing the mechanical properties and load-carrying capacity of fire-damaged concrete members [12]. The slurry infiltration process effectively reinforces the fibrous matrix, resulting in improved structural integrity and enhanced resistance to post-fire distress, such as cracking and spalling. This innovative application of SIFCON as a strengthening material after fire damage holds great potential for the development of resilient and durable infrastructure [13]. Ongoing research and advancements in this area continue to contribute to the evolution of fire-damaged concrete repair and rehabilitation methodologies.

SIFCON shell strengthening with a 3 cm thickness and hybrid fiber composition can significantly enhance the performance of NSC columns in terms of load-carrying capacity and energy absorption, albeit at the expense of reduced stiffness [14]. The flexural capacity of strengthened beams with SIFCON has been investigated by Marid and Vahidi [10]. Different failure modes were observed based on the beam strengthening method and steel reinforcement ratio. The study underscored the potential of SIFCON as a viable solution for improving the performance and longevity of reinforced concrete structures.

The behavior of solid and hollow slurry-infiltrated fiber concrete (SIFCON) columns considering the fiber shape, hollow ratio, and cross-sectional shape was studied by Khamees et al. [15]. Two sets of columns were tested: ones with hybrid fiber reinforcement and ones with 6% hooked end fiber reinforcement. The findings demonstrated that SIFCON columns perform well in terms of load carrying ability, ductility, and energy absorption capacity despite having a small cross-sectional area and longitudinal holes, particularly for hybrid fiber-reinforced columns.

Various types of fiber were used to study the effect of SIFCON laminates on frame structural strength [16]. SIFCON laminates decreased deflection values as thickness and fiber content increased. The results indicated that the failure of the structure can be delayed by using SIFCON laminates. In addition to the studies mentioned above, there are many other studies in which researchers used various types of strengthening materials. The studies are listed in Table 1.

Table 1. Types of strengthening materials used by the researchers in their studies

References	Type of strengthening
Vritesh & Asish [17]	Reinforced Concrete Jacketing (RCJ), Reinforced Concrete Wire Mesh Jacketing (RCWJ), and Steel Jacketing (SJ)
Suntharalingam et al. [18]	Use of Rockwool
Abdulghani & Jaafer [19]	Steel fibers and SIFCON
Salehi et al. [20]	Combining steel-BFRP bars and different BFRP sheet angles
Mohammed et al. [21]	Fiber-reinforced polymers (FRPS)
Yoo et al. [22]	Fiber-reinforced-polymer (FRP) sheet
Hashad et al. [23]	Epoxy-bonded steel plates
Warwar & Said [24]	Gypsum and plaster layers

Addressing the impact of different fiber sizes of SIFCON on the ultimate load capacity, stiffness, ductility, and absorption energy of the concrete elements could provide valuable insights into the potential for improving the performance of structural elements. Furthermore, evaluating the effectiveness of SIFCON and its comparative effects with CFRP technology on different concrete strength types is essential for understanding the versatility and applicability of these strengthening methods across varying concrete properties.

This research aims to explore the comparative effectiveness of these two strengthening materials by considering two parameters: two thicknesses for SIFCON (20 mm, 30 mm) and two thicknesses for CFRP (1.5 mm, 2.5mm). It covers two types of concrete (normal 25 MPa and high-strength 65 MPa) to evaluate the performance of these strengthening methods across different concrete compositions and strengths. Additionally, it delves into the performance characteristics of toughness, ductility, and stiffness associated with these strengthening methods, aiming to comprehensively evaluate their mechanical properties and behavior under varying loading conditions.

By addressing these parameters, the study seeks to contribute significantly to the body of knowledge related to structural rehabilitation and strengthening, ultimately illuminating robust and effective techniques for enhancing the performance of reinforced concrete structures.

2. Research Methodology

Figure 1, shows the flowchart of the research methodology through which the objectives of this study were achieved.

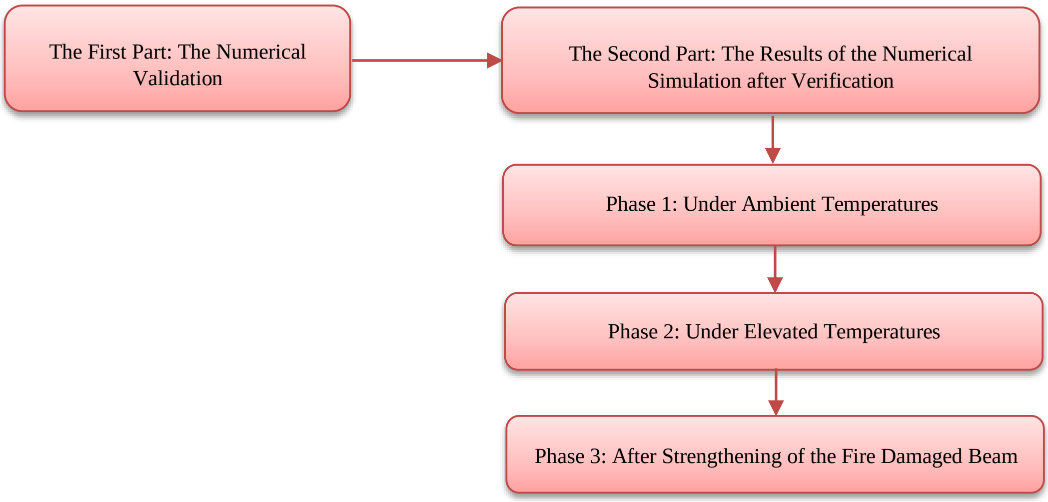

Figure 1. Flowchart of the methodology

3. Material and Methods

It is common to define both elastic and plastic phases to accurately capture the material behavior. The elastic phase of concrete, as with other isotropic materials, is typically characterized by two fundamental parameters: the modulus of elasticity and Poisson's ratio [25]. The modulus of elasticity reflects the material's stiffness, defining the relationship between stress and strain within the elastic range. It indicates how much a material will deform under a given amount of force. The Poisson's ratio, on the other hand, represents the material's response to lateral strain when it is under axial loading. It is a dimensionless parameter that describes the material's tendency to contract in the directions perpendicular to the applied force [24].

There are two models used to characterize the concrete plastic phase: the damaged plasticity model CDP and the concrete smeared cracks model. It is recommended to use the CDP model to characterize the plastic phase of quasi-brittle materials such as concrete because of its efficiency in predicting concrete response under various conditions, such as monolithic and repeated loadings, plain and reinforced concrete, and its application, which depends on the material loading rate [26-28]. The most important aspect of such a model is its ability to predict isotropic elasticity and also the isotropic tensile and compressive damaged plasticity to represent the inelastic part [29].

It's essential to accurately define the concrete damaged plasticity model parameters (CDP) in ABAQUS to capture the behavior of concrete under various loading conditions [30]. The five main parameters—angle of dilation, eccentricity, surface plasticity flow number, viscosity, and the ratio of biaxial compressive strength to the uniaxial compressive strength—play a critical role in shaping the failure surface envelope. These parameters are fundamental to capturing the complex behavior of concrete, particularly in the plastic phase [11]. Table 2 illustrates the parameters of the CDP failure surface.

Table 2. CDP material parameter for unfired concrete

Parameter	Selected value
Material model	CDP model
E, MPa	23500 MPa for C25 and 38000 MPa for C65
Possion's ratio	Varied according to the temperature
Dilation angel	30 for C25 MPa and 40 for C65
*Ecc	0.1
*Fb0/f_{c0}	1.16
*K	2/3
*Viscosity parameter	0.001

*As recommended by ABAQUS manual

Additionally, it should define the compressive and tensile behavior, including the inelastic compressive strength with the plastic strain curve and the inelastic stress with the cracking strain curve, beyond the cracking strength. These parameters are crucial for accurately modeling the behavior of concrete under both compression and tension [31].

Another two important curves required to be input to the CDP model are the uniaxial unconfined stress-strain behaviour under both compressive and tensile loading at ambient temperature (20 °C). Figure 2 clarifies the unconfined compressive stress-strain behavior of concrete in both normal and high-strength classes, providing valuable input for the model. The elastic part, characterized by the modulus of elasticity and Poisson's ratio, delineates the initial response of concrete to loading. Meanwhile, the plastic part, defined by the CDP model, captures the inelastic behavior of concrete under higher loads, encompassing both tensile and compressive responses.

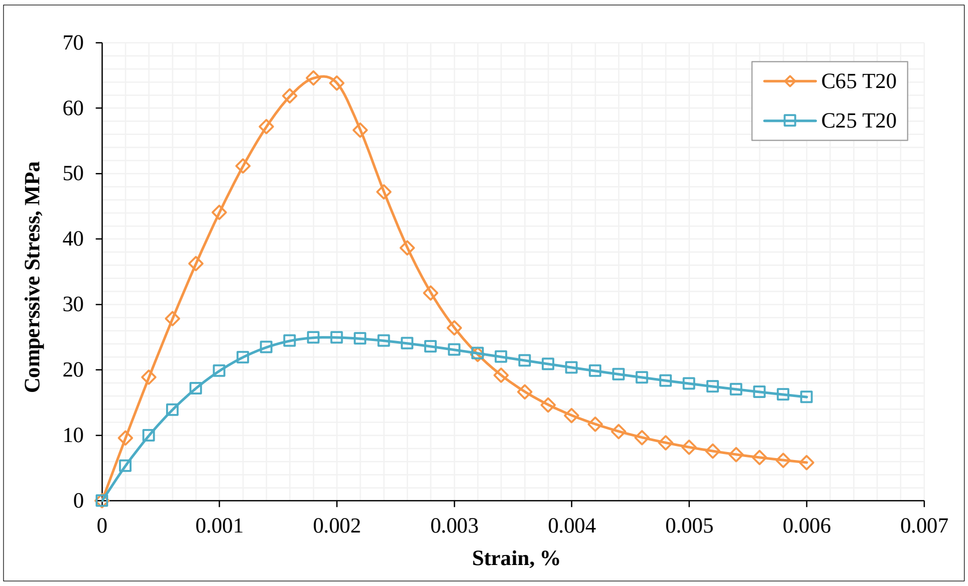

Figure 2. Uniaxial concrete compressive stress- strain at ambient temperature (20 °C) for normal (25 MPa) and high (65 MPa) strength concrete class

For steel material, generally, there are four stress strain models that are used to characterize its behavior: engineering stress strain, true or logarithmic stress-strain relation, elastic perfect plastic behavior, or bilinear elastic-plastic with hardening [32]. The built-in bilinear kinematic reinforcement model of ABAQUS was used to simulate reinforcement steel and the elastic modulus. For steel reinforcement rebar's, the elastic-perfect plastic behavior has been adopted in this study. Such behavior requires defining the elastic and plastic models with a minimum point at yielding, which corresponds to a zero-plastic strain. On the other side, the linear hardening of the plastic phase requires two points as a minimum: the yield point and the rapture point [33]. Other relations mentioned require defining more than two points in plastic behavior.

Finite Element Analysis and Modeling using ABAQUS was applied in this study. In general, the process includes three main phases, which are:

- Phase 1: modeling and simulating the reference samples (unfired concrete elements, without enhancement)
- Phase 2: simulating the concrete beam samples subjected to high temperatures without enhancement
- Phase 3: modeling and simulating the fired concrete beam after enhancement

While using ABAQUS, the following primary steps should be followed:

1-Modeling parts: use the appropriate modeling tools in ABAQUS, create a comprehensive 3D geometric model of the concrete elements.

2-Material properties: describe and define the characteristics of the concrete as well as any materials used as reinforcement, such as CFRP, SIFCON, steel, etc. These characteristics include elasticity, strength, failure criteria, and material behavior.

3-Assembly: assemble all the concrete structure's individual elements or components, including any reinforcements.

4-Step definition: specify the length of the simulation process, the kind of analysis (static, dynamic, or thermal), and the solver settings.

5-Constraints and interactions: describe the assembly's boundary conditions, limitations, and interactions between the various concrete element components.

6-Loading and boundary conditions: apply the proper loads, boundary conditions, and environmental influences (such as temperature variations) to simulate realistic operating conditions.

7-Predefined fields: specify any starting points that should be included in the model, such as temperature distribution, stress, and strain.

8-Job submission: use the specified settings and inputs, prepare and submit the simulation job for analysis.

4. FEM Results: Numerical Simulation Results of Concrete Elements under Different Conditions

4.1. Numerical Validation

Before starting any parametric investigation using the finite element simulation that validation with the previous experimental work be done. Therefore, a previous study by Cai et al. [34] has been adopted for the validation process, with geometrical configuration and material properties as clarified in Figures 3 and 4.

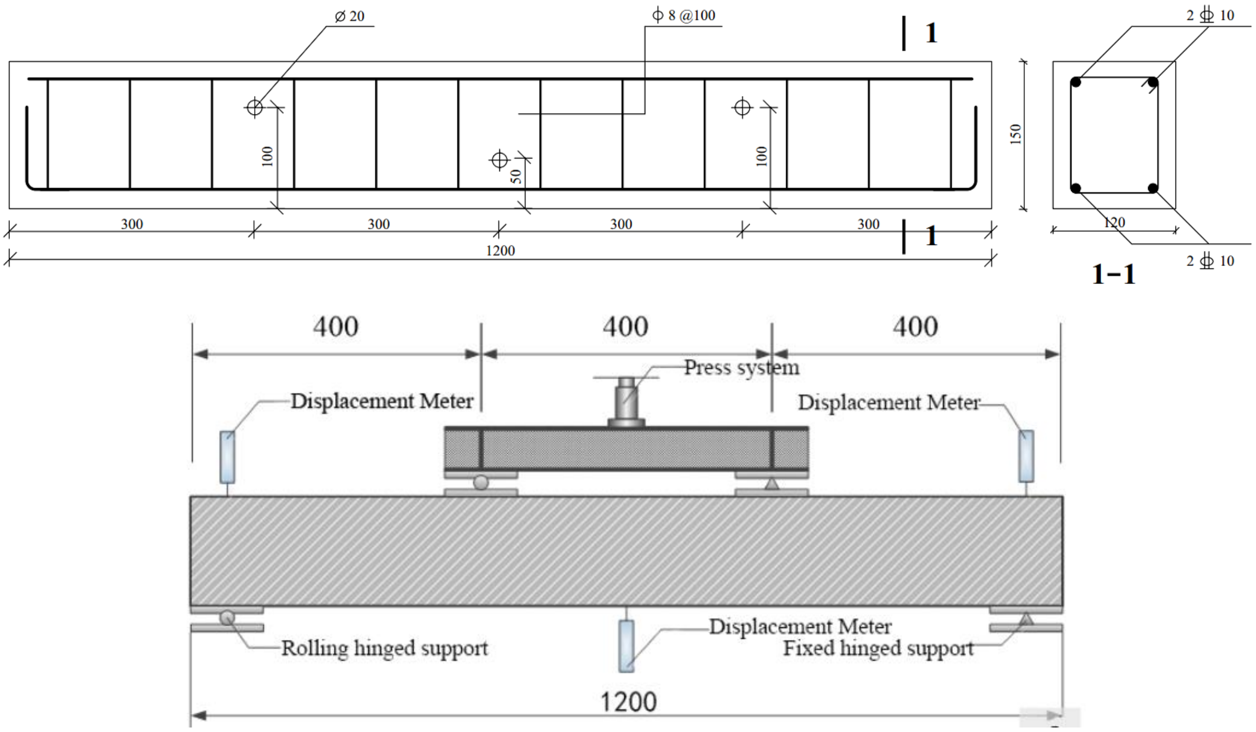

Figure 3. Geometric layout of the validated beam [34]

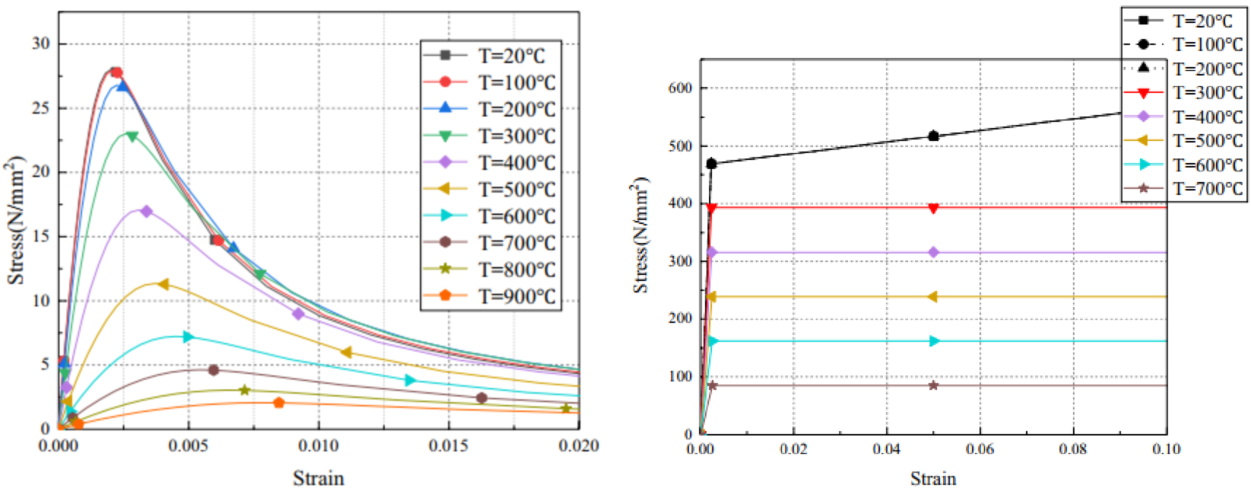

Figure 4. Properties of concrete and steel reinforcement of the validated research

In brief, the previously mentioned study was to investigate the effect of firing on the performance of the concrete beam after one hour of exposure to bringing [34]. All the data were geometrically modelled, and materials were defined, assembled, and loaded in ABAQUS.

The similarity between the numerical validation curves and the experimental test curves, as shown in Figures 5 and 6, suggests a strong correlation between the model and the real-world behavior of the concrete beams under both normal and fire-damaged conditions.

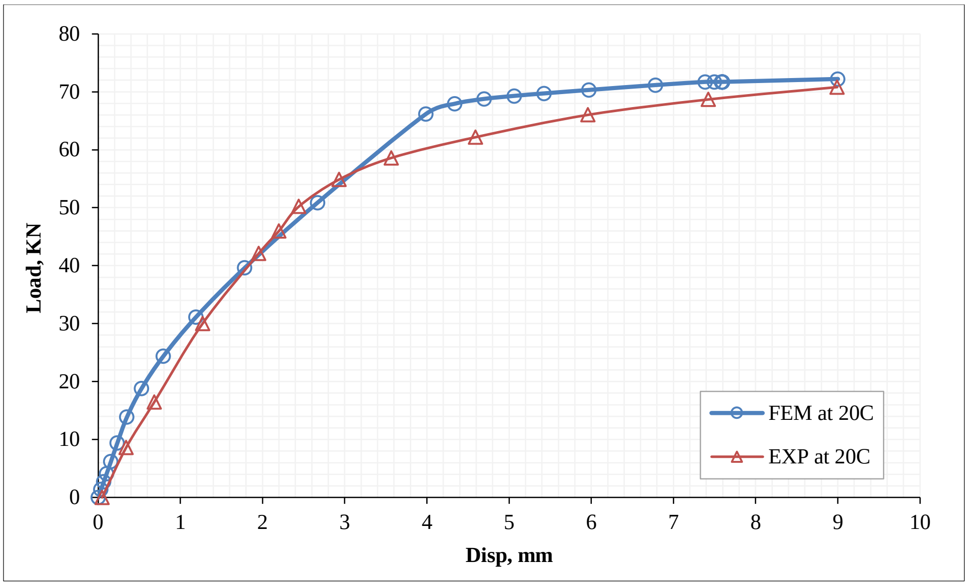

Figure 5. Experimental vs. numerical load-displacement curves at ambient temperatures

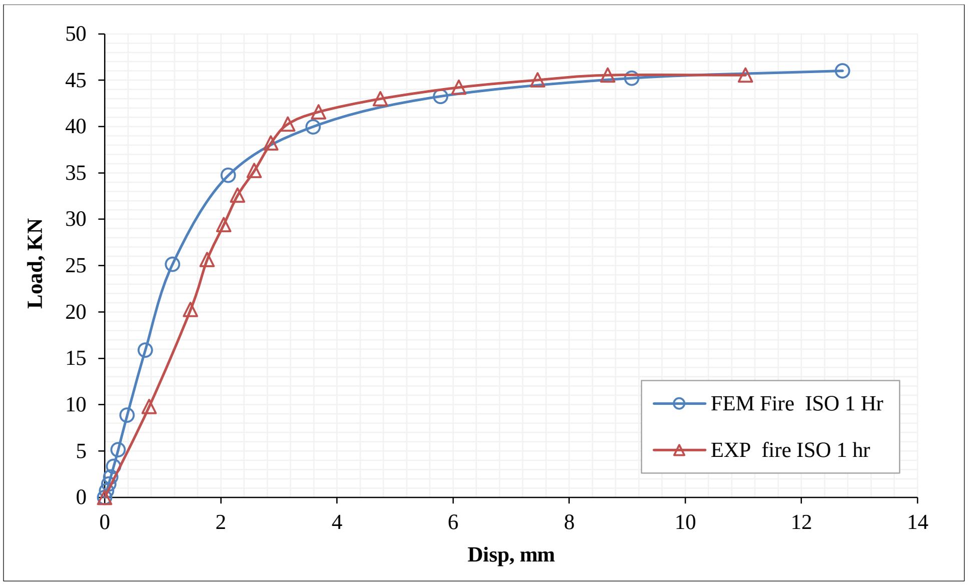

Figure 6.-Experimental vs. numerical load-displacement curves after 1-hour firing

The fact that the ultimate load-carrying capacity and the corresponding displacement values displayed an error percentage of less than 5% is indeed a significant validation outcome, indicating a high level of accuracy in the numerical simulations. The consistency of the curves' behaviors in both the elastic and plastic phases further strengthens the validation, especially in highlighting the similarities between the undamaged validated beam in the elastic phase and the plastic phase of the damaged beam.

These results provide confidence in the accuracy of the adopted concrete properties under various temperature degrees and the steel reinforcement properties, which are essential for initiating the parametric study of the concrete element (beam). With these properties established as accurate, they can serve as a solid foundation for investigating further damage cases, such as prolonged exposure to higher temperatures (more than 1-hour firing, or 2 hours).

Validation against this prior study helps ensure that the finite element model accurately represents the real-world behavior of the concrete beam under fire exposure. Through this validation process, any discrepancies between the simulated results and the experimental data can be identified and addressed, guaranteeing the reliability of subsequent parametric investigations. By aligning the simulation results with the experimental data from the previous study, the current research can build confidence in the finite element model's ability to capture the complex behavior of concrete beams under fire conditions. This rigorous validation process provides a solid foundation for the upcoming parametric study, enabling a deeper understanding of the effects of various parameters on the performance of fire-damaged concrete structures.

Levels of degradation and improvement in the elements' performance in terms of different flexural indices will be demonstrated, along with the behavior of the beam under various temperature conditions and repair processes. These details will be given and analyzed in detail. Table 3 shows that the beam was assigned a number based on the kind of concrete strength (high strength concrete (H), normal strength concrete (N), and type of strengthening (SIFCON (SX) and CFRP (CFx), where X is the layer thickness).

Table 3. Adopted Concrete members' designation

Beam dimension	Type of concrete	Beam designation	Type of strengthens	Configuration of strengthen
Beam with appreciate dimension (5.5×0.3×0.55) m	Normal concrete	B-R-N	-	-
	25 MPa (NSC)	B-F-N	-	-
		B-S20-N	SIFCON	20 mm
		B-S30-N	SIFCON	30 mm
		B-CF1.5-N	CFRP	one layer
		B-CF2.5-N	CFRP	two layer
	High concrete	B-R-H	-	-
	65 MPa (HSC)	B-F-H	-	-
		B-S20-H	SIFCON	20 mm
		B-S30-H	SIFCON	30 mm
		B-CF1.5-H	CFRP	one layer
		B-CF2.5-H	CFRP	two layer

4.2. Thermal Distribution Map on The Concrete Beam and Steel Reinforcement

As shown in Figure 7, isothermal curves have been created for the concrete beam to the ISO stranded fire curve during the thermal and heat transfer analysis in some essential specified areas. These places set at different depths along the cross-section midline: at the bottom surface, at the steel reinforcement, at the mid-depth and third quarter depth of beam. Observations revealed that following an hour of firing, the temperatures at the indicated points—from the bottom face to the top beam—were 42 °C, 310 °C, and 495 °C, respectively.

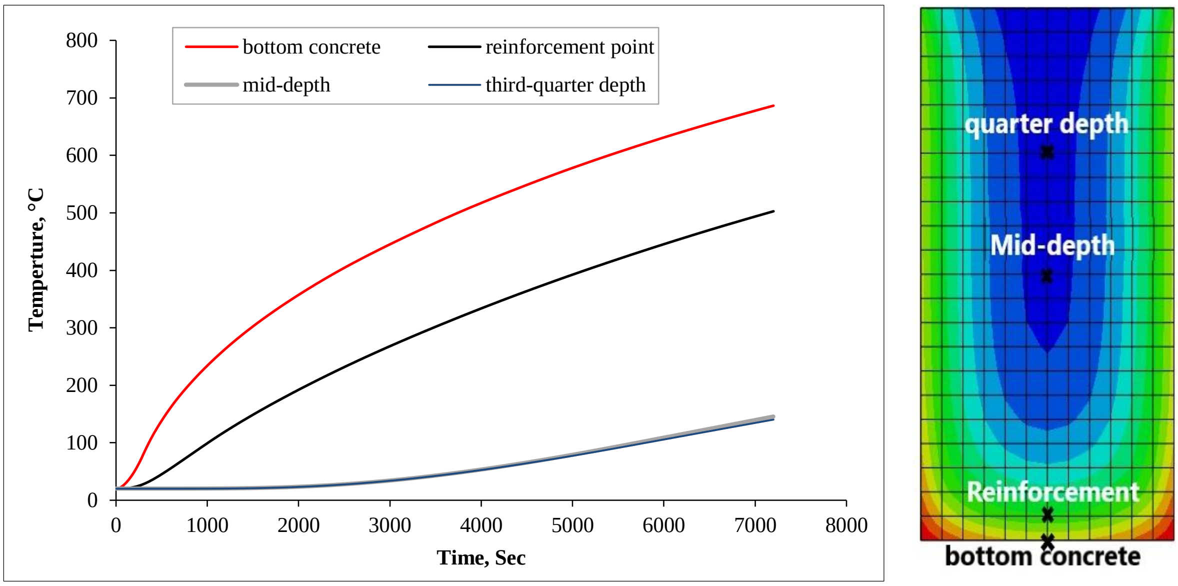

Figure 7. Isothermal curves at specified location in the beam cross section

The temperature readings for the aforementioned locations were 140 °C, 502 °C, and 686 °C after two hours in the same way. Furthermore, Figure 8 shows the temperature distribution of the beam cross section at the intervals of 30 minutes, 60 minutes, 1.5 hours, and 2 hours (a, b, c, and d). It should be mentioned that the thermal concentration at the corners of the beams was the highest, reaching 895 °C. In addition, the bottom longitudinal bars reached 528 °C after two hours, according to the three-dimensional representation of the temperature distribution on the steel reinforcement. The initial residual stress before to the mechanical load and strengthening phase was reflected in all of the temperature changes that were described.

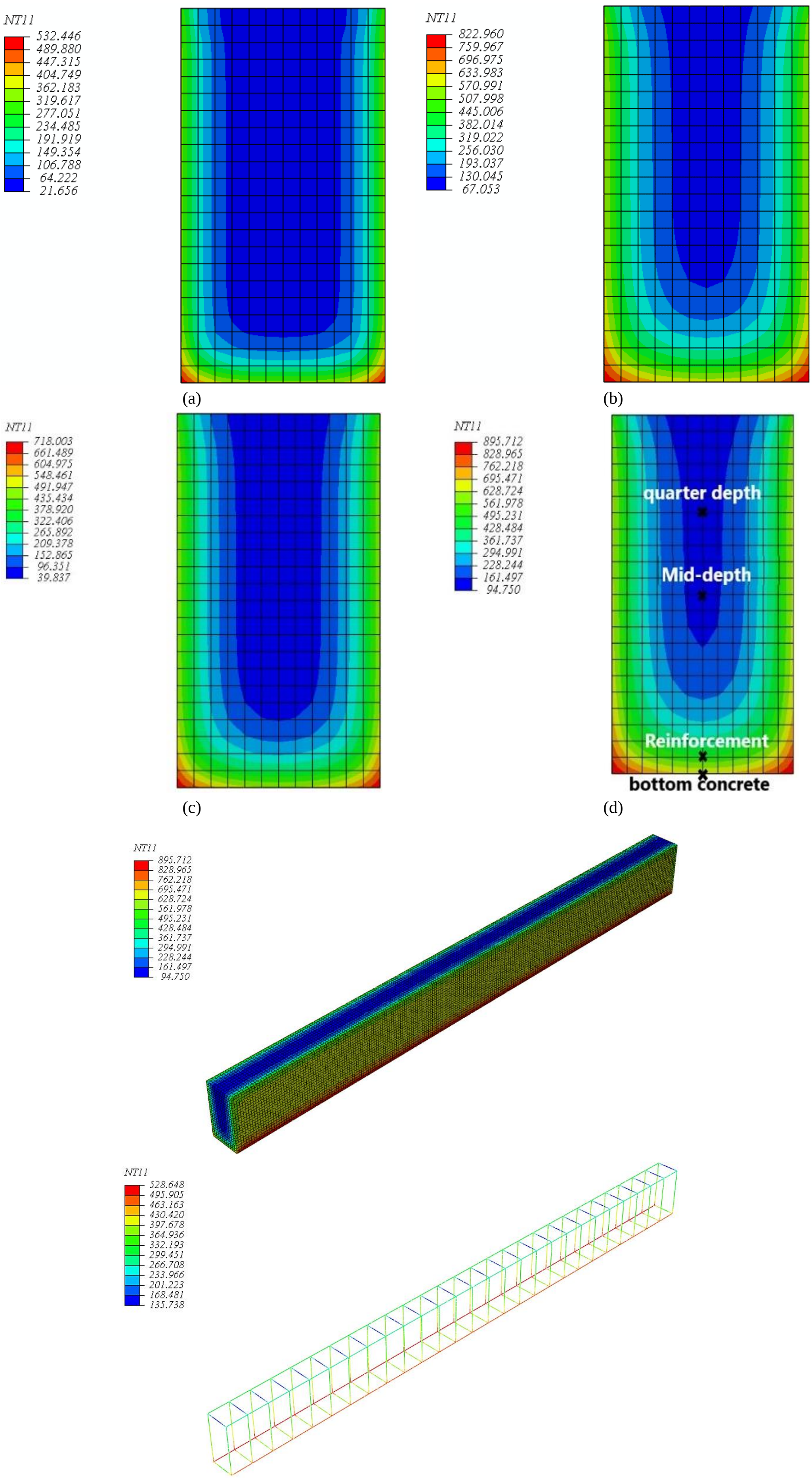

Figure 8. Temperature distribution on the beam cross section after a). Half of an hour, b). One hour, c). One and half of hour, d). 2 hours. In addition to a 3D view of temperature distribution on the beam and steel reinforcement

4.3. Behavior of the Concrete Beam under Ambient and Elevated Temperatures

Figures 9 and 10 show the load-midspan behavior for the mentioned concrete beam with typical concrete strength. The beam curves that are displayed are both before and after a two-hour firing. The undamaged model has thresholds in the form of elastic and service limits. The ABAQUS output feature of the plastic dispassion curve for the entire model yielded the obtained elastic limit. The initial cracking point is when the plastic dispassion energy begins to leak out. The temperature and flame begin to increase from the bottom face to the top one when fire incidents cause the temperature to rise [35].

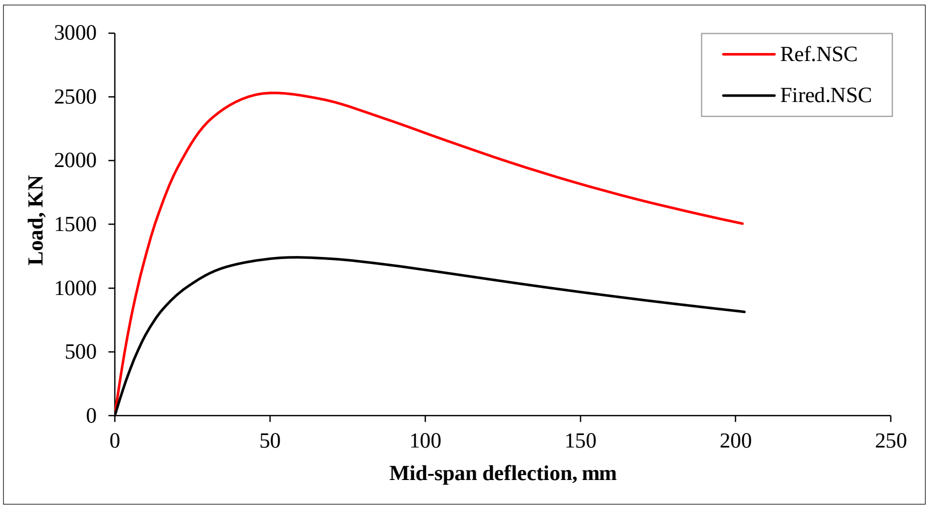

Figure 9. Load-displacement curves at ambient and elevated temperatures for the normal concrete strength class concrete

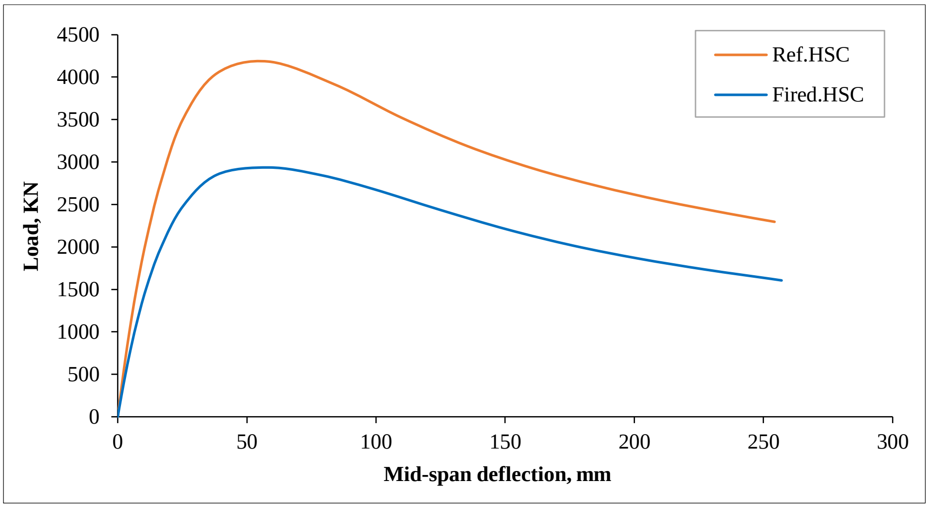

Figure 10. Load-displacement curves at ambient and elevated temperatures for the high concrete strength class concrete

The temperature and flame begin to increase from the bottom face to the top one when fire incidents cause the temperature to rise. On one side, the thermal gradient changes with time, and on the other, it varies with beam depth. The nature of the substance (thermal properties) of the concrete is the cause of this temperature variance. For example, the concrete cover may show 650 °C while the ambient temperature exceeds 950 °C, while the core remains below the limit of less than 100 °C. Even at a consistent rate, the temperature of the concrete core is still rising. While the compression zones—which are found at the base of the midspan and at the bottom of the span—represent the largest portion of the concrete load.

Even at a consistent rate, the temperature of the concrete core is still rising. The steel reinforcement is still subject to the most significant temperature-raising effect, which is causing a noticeable reduction in the overall behavior of the beam, even though the compression zones—located at the top of the support in the case of fixed support and at the bottom of the midspan—represent the most significant portion of the concrete load.

Figure 11 shows the load capacity results for the reference and fired normal and high-strength concrete beams. It is clear that the normal concrete's load carrying capacity was significantly lower than the high-class concrete's, which is estimated to be around 50% and 30% for each type of concrete, respectively. Put another way, raising the concrete's compressive strength to 250% will result in a roughly 237% increase in the beam's resistance to load carrying capacity.

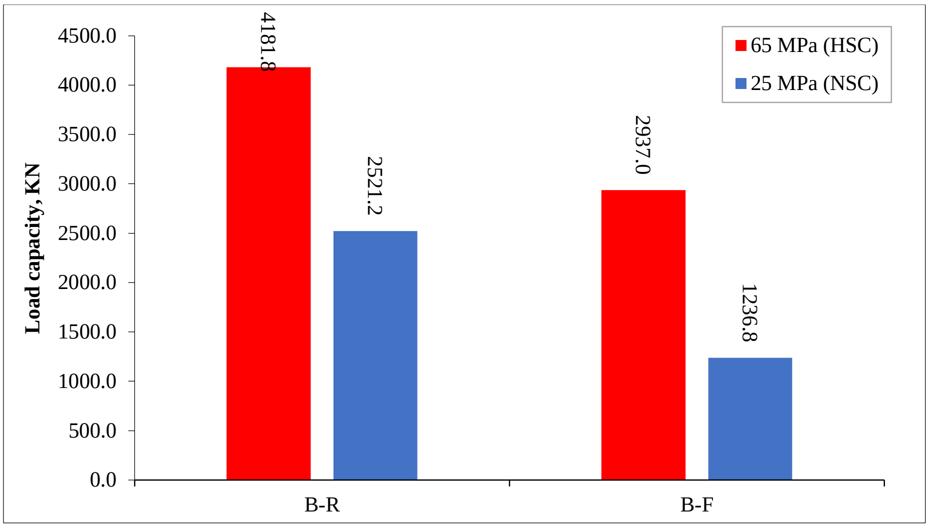

Figure 11. Ultimate load capacity of the reference and fire damaged concrete beam

The impact of elevated temperatures on flexural indices, such as stiffness, ductility, and toughness (absorption energy), is clearly depicted in Figures 12 to 14. The observed deterioration in stiffness for both normal and high-strength concrete classes, at around 48% and 62% respectively, indicates a significant reduction due to the effects of elevated temperatures. Similarly, in terms of ductility, reductions of 34% and 75.75% were noted, further underlining the impact of high temperatures on the mechanical properties of the concrete beams.

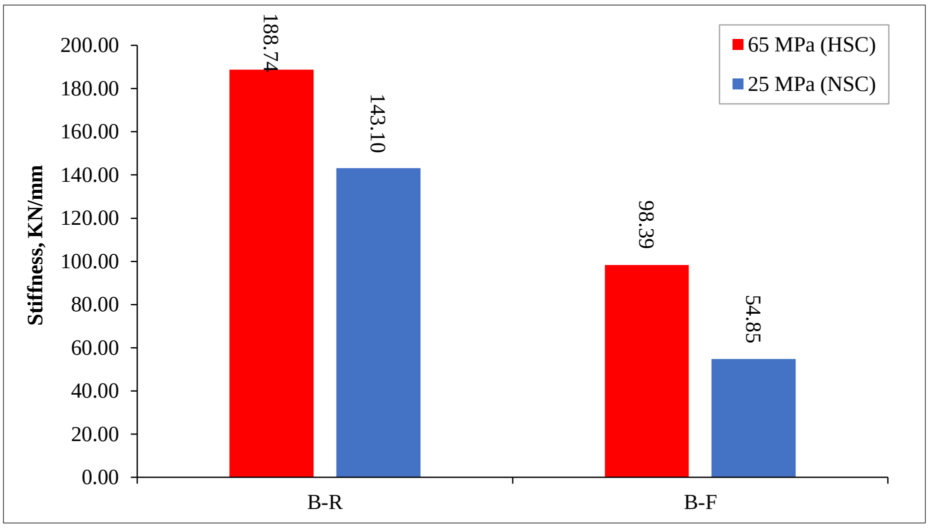

Figure 12. Effect of high temperatures on stiffness of the normal and high strength class concrete beam

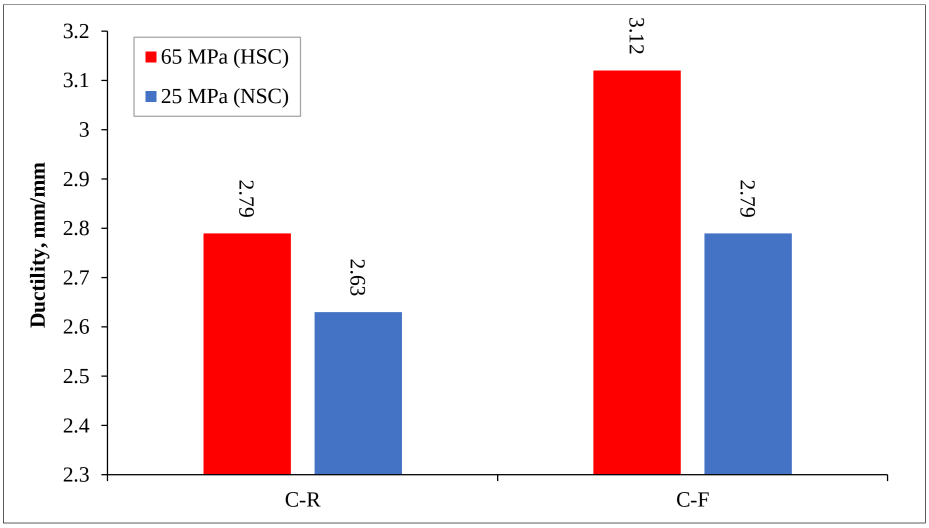

Figure 13. Effect of high temperatures on the ductility of the normal and high strength class concrete beam

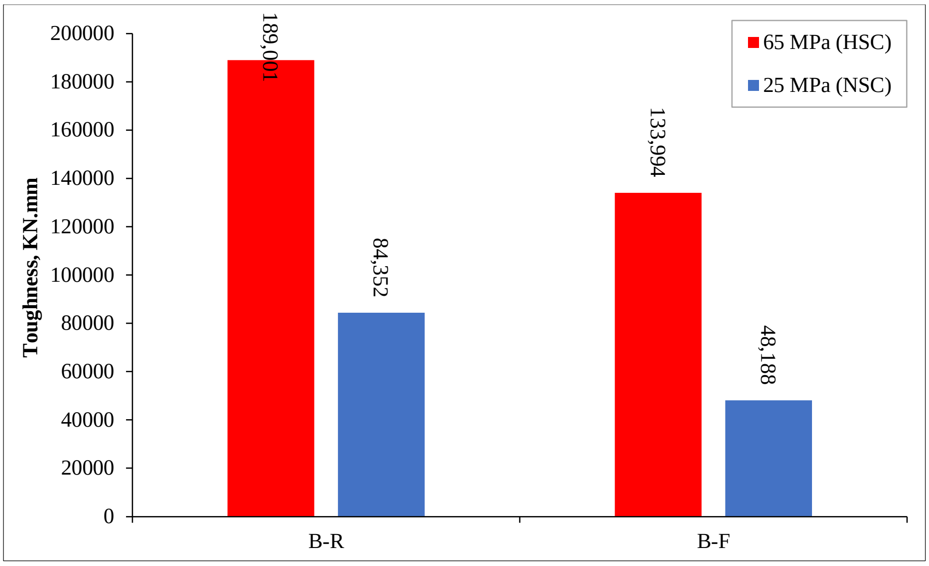

Figure 14. Effect of high temperatures on toughness performance of normal and high strength concrete beam

In other words, if the concrete compressive strength of the beam were increased, the fire resistance would increase by roughly 181% based on the stiffness index. Conversely, raising the compressive strength of concrete by 250% would result in an approximately 111% increase in fire resistance according to the ductility index. It should be mentioned that when fire was applied to concrete, its ductility increased.

Figure 14 illustrates how high temperatures affect the beam's toughness, or its ability to absorb energy until it fails. The Figure shows that the absorption energy values for the normal and high strength classes were lowered by approximately 42.8% and 29.1%, respectively, following two hours of firing on the concrete beam. This means that the fire resistance in terms of the absorption energy index would increase by roughly 278% if the concrete compressive strength of the beam increased by 250%

4.4. Behavior of the Fire-damaged Concrete Beam after Strengthening with CFRP Layer

Figure 15 shows the load-mid-span deflection behavior of normal strength-class concrete that was strengthened using two different CFRP wrapping sheet thicknesses. When compared to fire-damaged beams, it is evident that wrapping normal concrete beams with 1.5 mm and 2.5 mm CFRP thicknesses successfully recovers the maximum load carrying capacity.

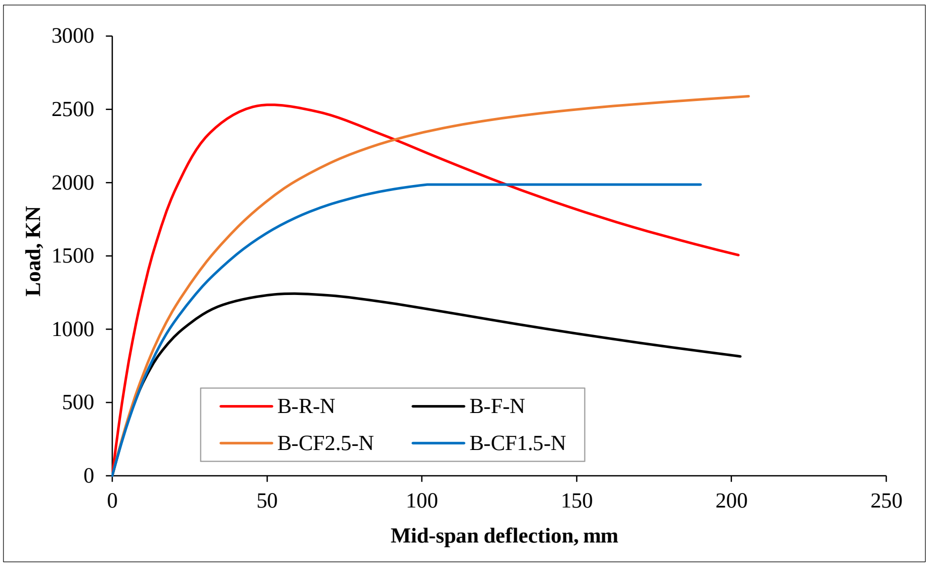

Figure 15. Effect of beam's strengthening with two various CFRP jacket thickness on the load- mid span displacement behavior of normal strength concrete

The reference undamaged beam and the 1.5 mm CFRP-strengthened beam are still incomparable. as opposed to the 2.5 mm CFRP strengthening, which has effectively restored the load-carrying capacity.

Furthermore, the reference beam's value and the fire-damaged beam model were both comparable to the initial stiffness of the strengthened beam with CFRP. In addition, the reinforced beams' ductility was greater than that of the reference and fire-damaged beams.

Figure 16 shows the load-mid-span deflection behavior for the high-strength concrete after it was strengthened with two different CFRP wrapping sheet thicknesses. When comparing the maximum load-carrying capacity of the concrete beam with that of a fire-damaged beam, it is evident that the CFRP jacket (for both thicknesses) improved the beam's maximum capacity. The reference, undamaged beam, cannot be compared to any of the enhanced beams. Additionally, the reference and the fire-damaged beam were at different points in the initial stiffening of the CFRP-strengthened beams. Furthermore, the strengthened beams had a higher degree of ductility than the reference and fire-damaged beams.

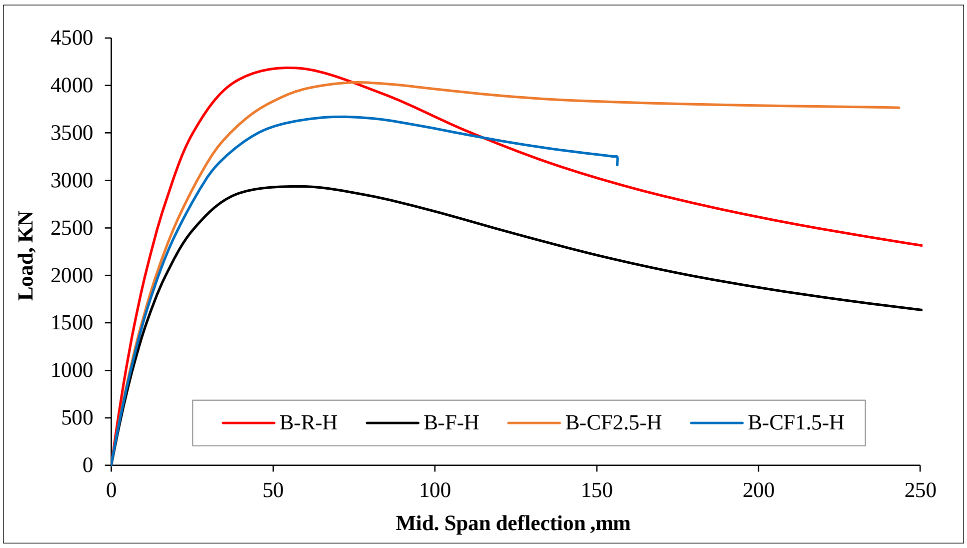

Figure 16. Effect of beam's strengthening with two various CFRP jacket thickness on the load- mid span displacement behavior of high strength concrete

For normal-strength concrete and in terms of the load carrying capacity as clarified in Figure 17, compared with the fire-damaged beam model, the load carrying capacities were enhanced by about 200% and 160% for 2.5 mm and 1.5 mm CFRP-strengthened beams, respectively. While comparing the results with the reference normal-strength beam, only the 2.5 mm CFRP-strengthened beam successfully achieved the same capacity.

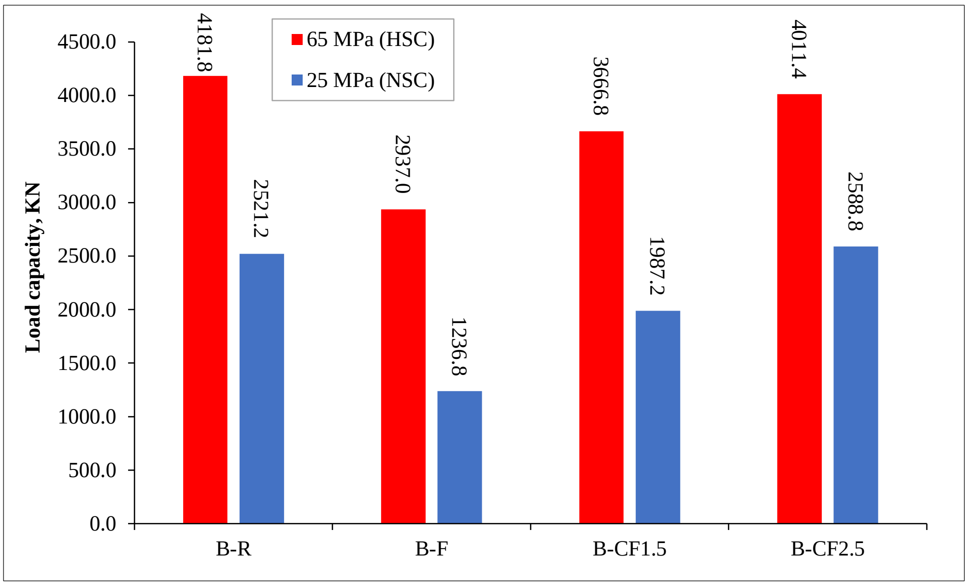

Figure 17. Load carrying capacity comparison between the CFRP strengthened beams and the reference and fire damaged beams

On the other side, the 1.5 mm and 2.5 mm CFRP-strengthened beams have reflected load capacities higher than the fire-damaged beam by about 123% and 136%, respectively. While only the 2.5 mm CFRP-strength beam was comparable to the reference high-strength beam.

The initial stiffness values of various beam types are illustrated in Figure 18. It is clearly observed that increasing CFRP sheet thickness resulted in a noticeable improvement estimated at about 201% and 125% for 1.5 mm and 2.5 mm for normal CFRP-strengthened beams, respectively, when compared with fire-damaged beams. While an enhancement in the stiffness was found to be approximately the same and higher than the fire-damaged beam by about 150%, it was still insufficient to capture the value of the reference high-strength beam.

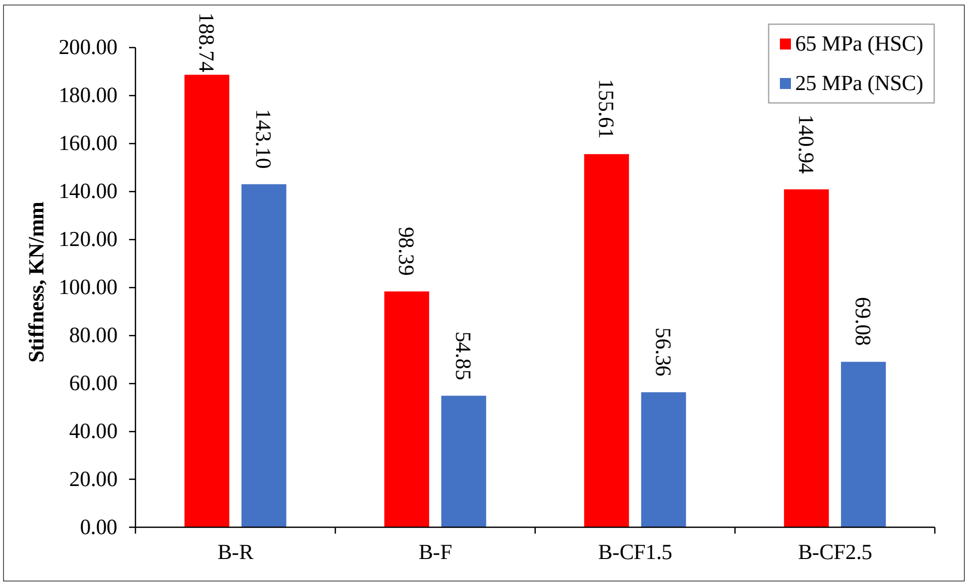

Figure 18. Stiffness performance of CFRP wrapped beams

Figure 19 shows the results, which indicate that the use of CFRP as a strengthening material can be highly effective in enhancing the ductility index of fire-damaged concrete beams. The thicker the CFRP layer, the greater the improvement in ductility. This demonstrates the potential of CFRP strengthening techniques for restoring or even surpassing the original ductility of fire-damaged beams.

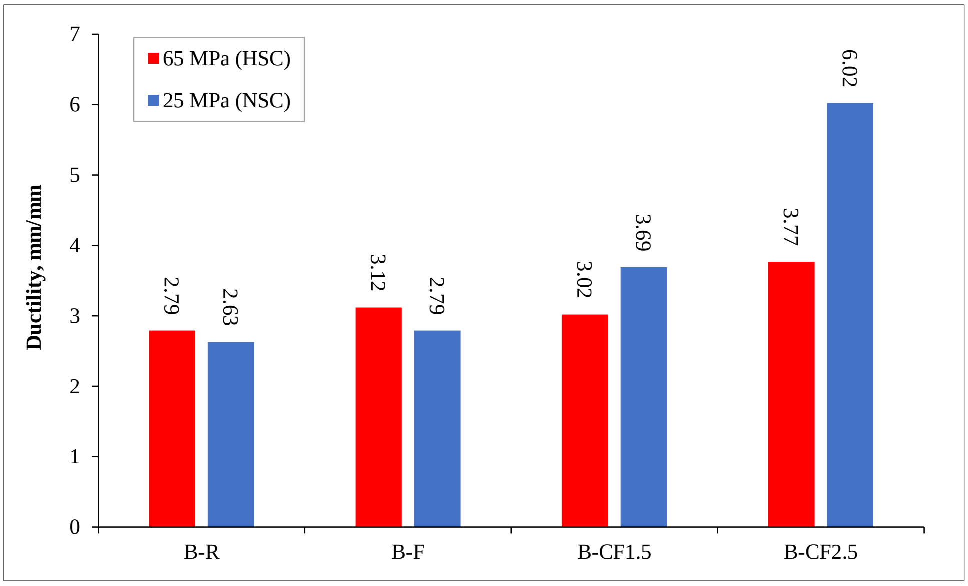

Figure 19. Ductility performance of CFRP strengthened beams

However, for high-strength concrete beams, the same as previously discussed for normal concrete beams, although with reduced enhancement percentages, for CFRP layer thicknesses of 1.5 mm and 2.5 mm, the ductility values have generally increased by roughly 105% and 165%, respectively.

In concrete beams with normal strength, CFRP generally has a bigger effect on the beam's ductility performance than it does in beams with high strength.

Figure 20 illustrates and compares the fracture energy of the CFRP-strengthened beams for both concrete classes with that of the reference and fire-damaged beams.

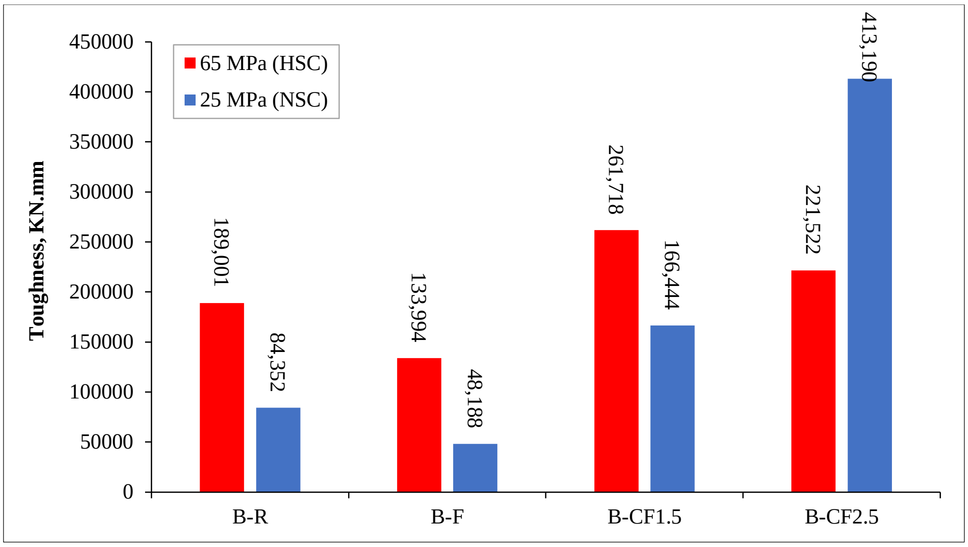

Figure 20. Toughness performance of CFRP strengthened beams

These findings highlight the effectiveness of CFRP as a strengthening material for increasing the toughness and overall structural performance of fire-damaged concrete beams. The thicker CFRP layer (2.5 mm) showed a greater improvement in fracture energy compared to the thinner layer (1.5 mm), indicating that the thickness of the CFRP significantly influences the level of enhancement.

Overall, the results suggest that CFRP-strengthened beams have exhibited substantial improvements in fracture energy when compared to both fire-damaged beams and the reference (undamaged) beams. This indicates the potential of CFRP strengthening to restore and enhance the structural integrity of fire-damaged concrete members. The 1.5 mm and 2.5 mm CFRP-strengthened beams had reflected toughness abilities higher than the fire-damaged beam by approximately 195% and 165%, respectively, in the same previously indicated data and for high-strength concrete classes. In addition, the strengthened beam's toughness was roughly 138% and 117% higher, respectively, than that of the reference undamaged beam.

Overall, in terms of toughness and ductility indices, the results indicated that the impact of the CFRP wrapping contribution is greater in the normal-strength concrete than the high-strength concrete.

4.5. Behavior of Fire-damaged Concrete Beams Strengthened with the SIFCON Layer

Figure 21 illustrates the load-displacement behavior of normal-strength, SIFCON-treated beams with two different jacket thicknesses (20 mm and 30 mm) along the side and bottom faces of the beam. When comparing the SIFCON-treated beams to the fire-damaged beam, it is evident that noticeable enhancement has occurred; however, the reference beam behavior is still unachievable. The outcome has sufficiently improved load capacity, stiffness, and toughness when compared to the fire-damaged beam. In contrast to the reference beam, there was less ductility.

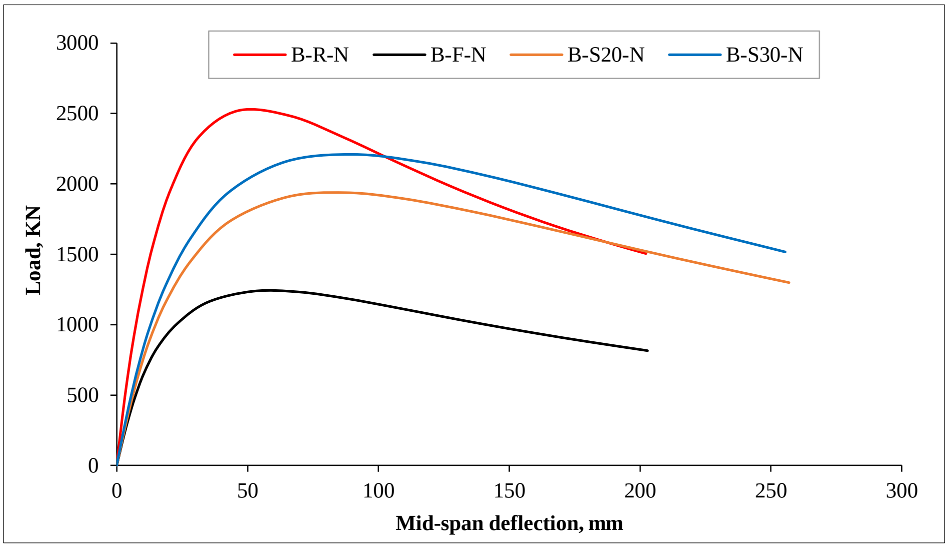

Figure 21. Effect of beam's strengthening with SIFCON jacket on the load- mid span displacement behavior of normal strength concrete beams

Compared to normal-strength beams, high-strength concrete beams treated with SIFCON exhibited different behavior. Overall, as shown in Figure 22, the ascending portion of high-strength, SIFCON-treated members was stiffer than fire-damaged beams in terms of the load displacement behavior; nonetheless, among the other beams, the reference high-strength beams remained the governing ones.

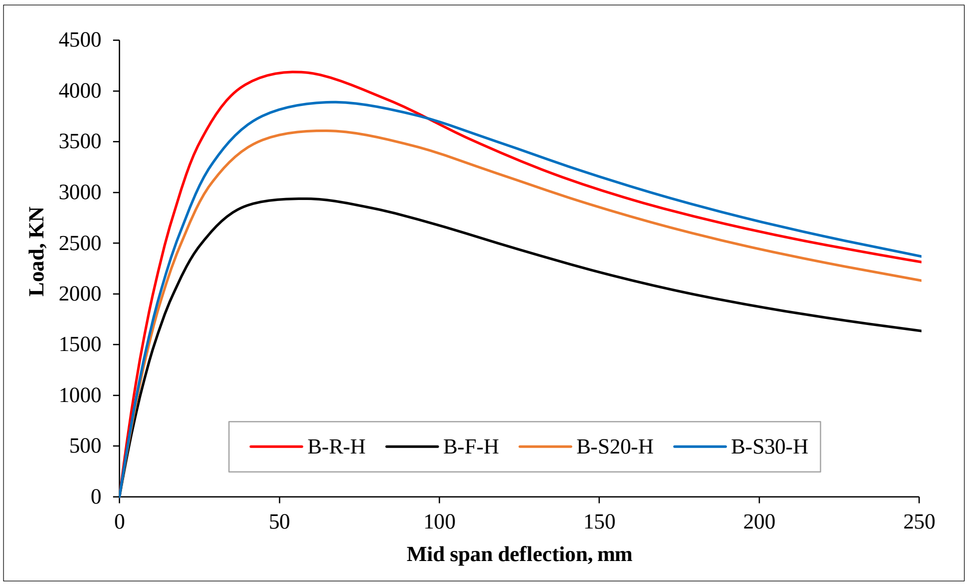

Figure 22. Effect of beam's strengthening with SIFCON jacket on the load- mid span displacement behavior of high strength concrete beams

It is also evident that increasing the thickness of the SIFCON jacket does not significantly affect stiffness or load-carrying capacity, as will be covered in more detail in the following subsections. As a result, the reinforced beam's ductility was reduced, but its toughness was increased.

For high-strength concrete in terms of the load carrying capacity, as clarified in Figure 23, and compared with the fire-damaged beam model, the load carrying capacities were improved by about 122% and 132% for 20 mm and 30 mm SIFCON-treated beams, respectively. While comparing the results with the reference normal strength beam, both of the previously mentioned beams decreased, but they were comparable. On the other side, the normal-strength concrete beams treated with SIFCON layers behaved in the same manner, with percentages of 156% and 174% for 20 mm and 30 mm layer thickness, respectively.

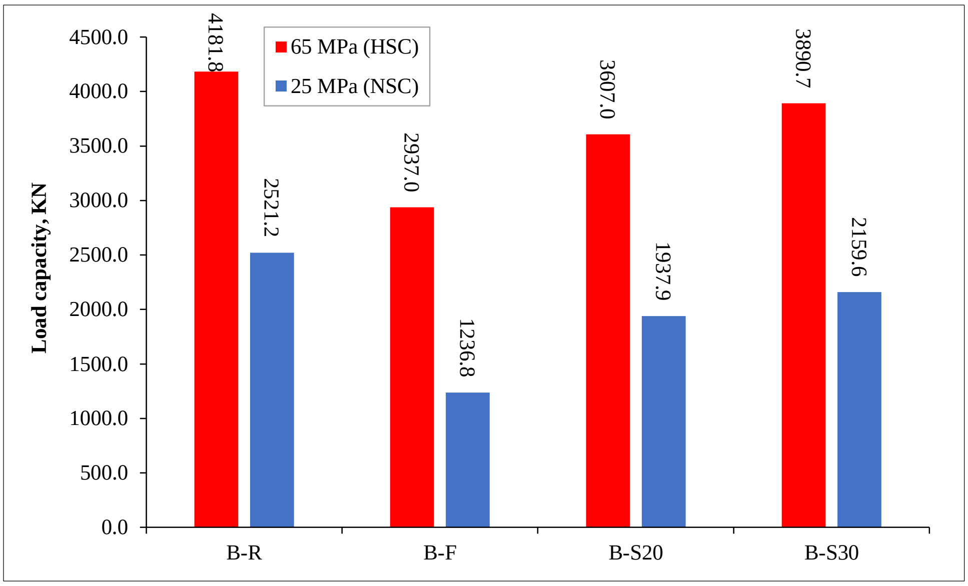

Figure 23. Load capacity performance of SIFCON jacket treated beams

Overall, increasing the SIFCON layer thickness by about 150% (from 20 mm to 30 mm) and treating the concrete beams with the SIFCON jacket layer have improved the load-carrying capacity by about 122%–174%.

In Figure 24, the stiffness values of beams treated with SIFCON are shown. The results indicate that there was a discernible increase in stiffness values for both concrete strength classes with increasing SIFCON layer thickness. Because both the 20 mm and 30 mm jacket thicknesses raised the reflected value of enhancement by around 150% when compared with a fire-damaged beam, the results demonstrated that increasing SIFCON layer thickness had no effect on stiffness for concrete beams of normal strength. For 20 mm and 30 mm SIFCON thicknesses for high-strength concrete beams, an approximate 110% and 133% increase in stiffness was reported; nevertheless, this improvement was not enough to match the value of the reference high-strength beam.

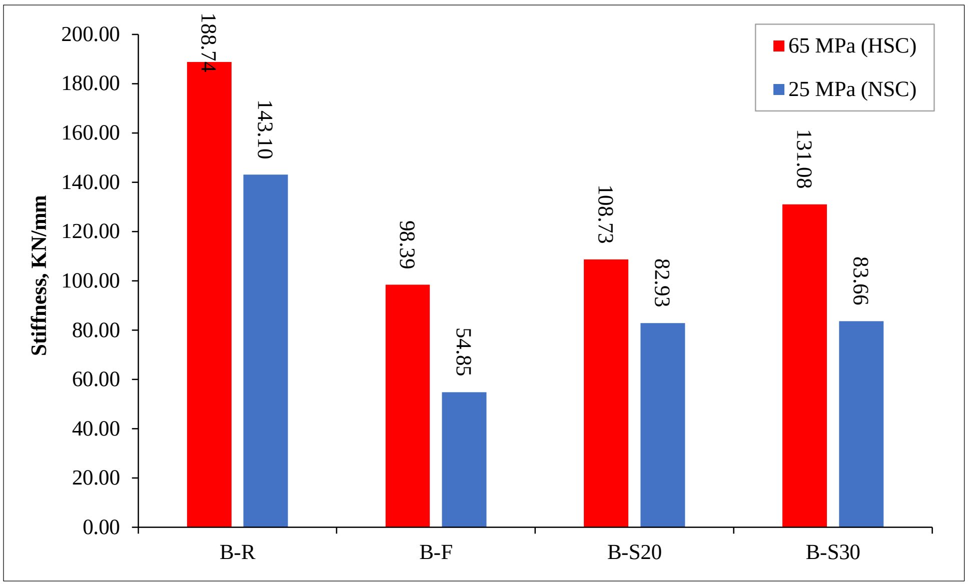

Figure 24. Stiffness performance of SIFCON jacket treated beams

Figure 25 shows the ductility results of the beams treated with SIFCON. For both concrete strength classes, there was often a slight decrease in ductility value with increasing SIFCON layer thickness. Additionally, for both concrete strength classes, the reference and fire-damaged beams had lower ductility values than the treated beams with SIFCON.

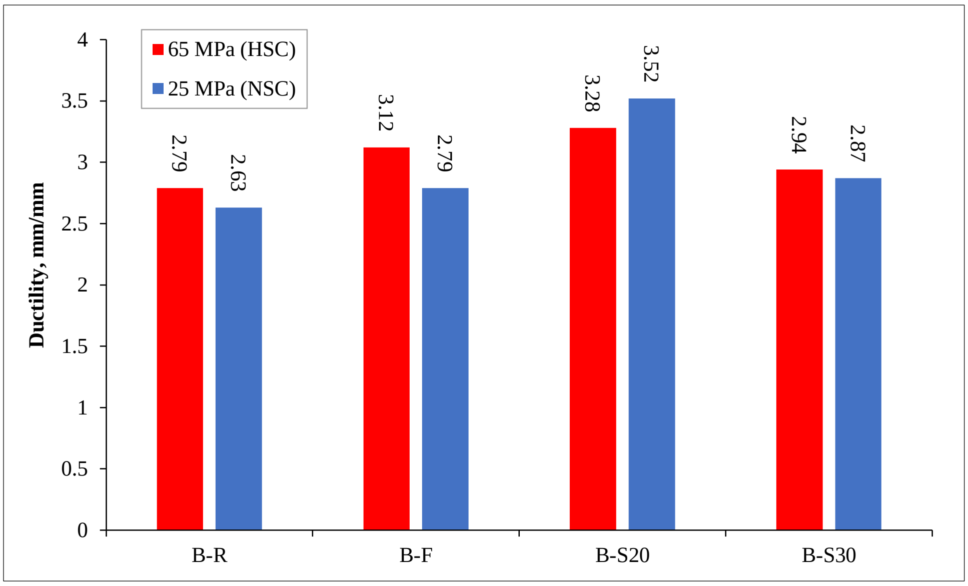

Figure 25. Ductility performance of SIFCON jacket treated beams

Generally speaking, a small variation in the ductility value was observed in the ranges of 2.78–3.52 and 3.12–3.28 for normal and high-strength concrete beams, respectively.

The fracture energy of the SIFCON-treated beams for both concrete classes is shown in Figure 26 and compared with that of the reference and fire-damaged beams. When normal-strength concrete was compared to the fire-damaged beam model, the toughness values increased by approximately 273% and 323%, respectively, for thicknesses of 20 mm and 30 mm SIFCON. The 20 and 30 mm SIFCON-strengthened beams had reflected toughness capabilities higher than the fire-damaged beam by approximately 135% and 146%, respectively, in the same previously indicated statistics and for high-strength concrete classes. Furthermore, the reference undamaged beam's toughness was lower than that of the augmented beam.

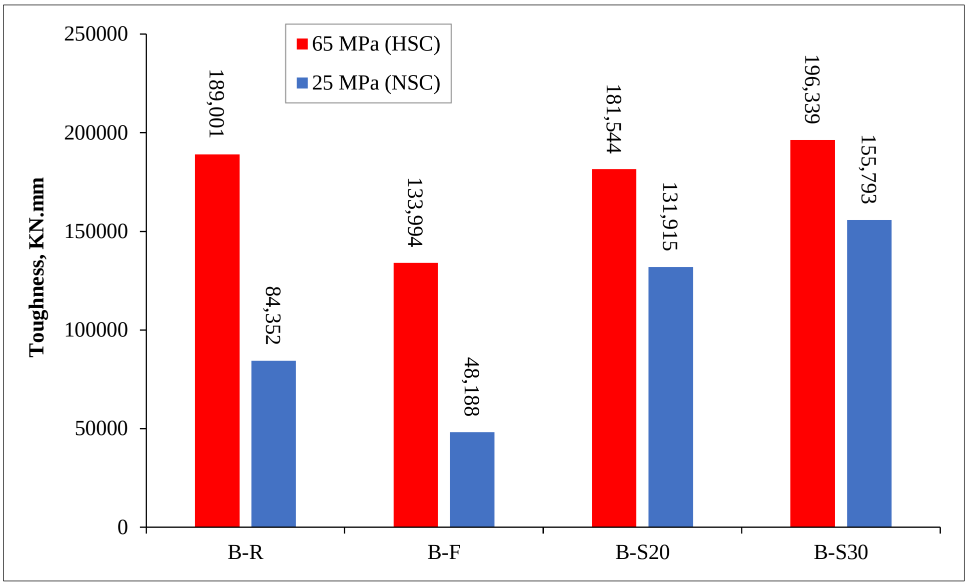

Figure 26. Toughness performance of SIFCON jacket treated beams

Table 4 provides a summary of how CFRP and SIFCON are used as efficient reinforcement and repair techniques to enhance the properties of different reinforced concrete members both before and after exposure to high temperatures. For the structural element and both types of concrete (NSC and HSC), the indicators (stiffness, ductility, and toughness) were investigated at each of the three stages of work.

Table 4. The effect of high temperature on Stiffness, Ductility and Toughness indicators

	Stiffness index		Ductility index		Toughness index	
	NSC	**HSC**	**NSC**	**HSC**	**NSC**	**HSC**
R	143.10	188.74	2.63	2.79	84.352	189.001
F	54.85	98.39	2.79	3.12	48.188	133.99
CFRP 1.5	56.36	155.61	3.69	3.02	166.444	261.718
CFRP 2.5	69.08	140.94	6.02	3.77	413.190	221.522
SFCON 20	82.93	108.73	3.52	3.28	131.915	181.544
SIFCON 30	83.66	131.08	2.87	2.94	155.793	196.339

In the case of reference, the concrete member denoted by (R) is considered undamaged, whereas (F) denotes the concrete member following exposure to fire.

Accordingly, after a comprehensive and deep study of this case, the following results can be drawn for beam:

- By increasing the thickness of the SIFCON layer from 20 mm to 30 mm by approximately 150%, the NSC beam's ability to carry loads was enhanced by approximately 122%–174%. By applying 20 mm and 30 mm SIFCON layer thicknesses to the fire-damaged HSC beam, the load capacity is increased by approximately 122% and 132%, respectively, in comparison to the fire-damaged beam. As for the 2.5 mm and 1.5 mm CFRP-strengthened NSC beams, respectively, the increase in load-carrying capabilities was almost 200% and 160%.
- Around 123% and 136%, respectively, more load capacity was reflected by the 1.5 mm and 2.5 mm CFRP-strengthened HSC beams than by the fire-damaged beam.
- The stiffness values of both normal and high-strength concrete beams showed a discernible improvement with increasing SIFCON layer thickness, and the strengthening CFRP in HSC beams resulted in an enhancement in stiffness that is approximately 150% greater than the fire-damaged beam. On the other hand, an increase in stiffness for NSC beams was found to be roughly equal.
- In both concrete strength classes, the treated beams with SIFCON exhibited greater ductility values than the reference and fire-damaged beams. Although CFRP affects the ductility performance of the concrete beam in the normal-strength class more so than in the high-strength class.

- The findings showed that increasing the thickness of the SIFCON layer by roughly 150% improved the toughness of the beam; the NSC beam had a larger SIFCON contribution than the HSC beam. Compared to the fire-damaged beam type, the CFRP-strengthened members have appropriate improvements for normal-strength concrete. Additionally, the strengthened beams' toughness in high-strength concrete was roughly 138% and 117% higher, respectively, than that of the reference, undamaged beam.

5. Conclusions

The behavior of fire-damaged RC beams before and after strengthening has been modeled and studied. Normal C25 MPa and high-strength C65 MPa concrete were considered. The modeled parts were subjected to the standard ISO fire curve with the aid of finite element simulation using ABAQUS software. Two types of post-fire strengthening were used after exposing the concrete elements to the fire effect: SIFCON with different fiber sizes and CFRP sheets with different thicknesses. All the adopted material properties and failure theories were adopted from previous studies after validation. In summary, the key conclusions are:

- For the normal-strength concrete beam, the CFRP repair with a 2.5-mm thickness improved the load-carrying capacities by 200% compared to the damaged beam. This was the highest improvement of all the repair techniques studied.
- For the high-strength concrete beam, the 2.5-mm-thick CFRP repair improved load-carrying capacities by 136% compared to the damaged beam; this was the highest improvement achieved.

This means that the CFRP strengthening technique was better than the SIFCON strengthening technique in terms of the load-carrying capacities of both types of concrete.

6. Declarations

6.1. Author Contributions

Conceptualization, A.E. and H.A.; methodology, A.E. and H.A.; software, H.A.; validation, A.E. and H.A.; formal analysis, H.A.; investigation, H.A.; resources, H.A.; data curation, H.A.; writing—original draft preparation, H.A.; writing—review and editing, A.E.; supervision, A.E. All authors have read and agreed to the published version of the manuscript.

6.2. Data Availability Statement

The data presented in this study are available in the article.

6.3. Funding

This study has been supported by the RUDN University Strategic Academic Leadership Program.

6.4. Conflicts of Interest

The authors declare no conflict of interest.

7. References

[1] Liu, T., Wang, H., Zou, D., Long, X., Miah, M. J., & Li, Y. (2023). Strength recovery of thermally damaged high-performance concrete subjected to post-fire carbonation curing. Cement and Concrete Composites, 143, 105273. doi:10.1016/j.cemconcomp.2023.105273.

[2] Abdalla, A. A., & Karim, D. F. R. (2022). Repairing Materials for Different Post Fire - Damaged Structural Concrete Members: A Critical Review. Construction, 2(2), 56–64. doi:10.15282/construction.v2i2.8660.

[3] Agrawal, A., & Kodur, V. K. R. (2020). A Novel Experimental Approach for Evaluating Residual Capacity of Fire Damaged Concrete Members. Fire Technology, 56(2), 715–735. doi:10.1007/s10694-019-00900-1.

[4] Alzamili, H. H., & Elsheikh, A. M. (2023). Performance of reinforced concrete elements retrofitted with SIFCON under elevated temperatures. Al-Qadisiyah Journal for Engineering Sciences, 16(1), 53–57. doi:10.30772/qjes.v16i1.969.

[5] Zhou, J., & Wang, L. (2019). Repair of Fire-Damaged Reinforced Concrete Members with Axial Load: A Review. Sustainability (Switzerland), 11(4), 963. doi:10.3390/su11040963.

[6] Naqvi, S. A. (2021). Flexural Strengthening of Two-Way Slabs Using CFRP External Laminates. Master Thesis, University of Texas, Arlington, United States.

[7] Abadel, A. A., Abbas, H., Alshaikh, I. M. H., sennah, K., Tuladhar, R., Altheeb, A., & Alamri, M. (2023). Experimental study on the effects of external strengthening and elevated temperature on the shear behavior of ultra-high-performance fiber-reinforced concrete deep beams. In Structures (Vol. 49, pp. 943–957). Elsevier. doi:10.1016/j.istruc.2023.02.004.

[8] Al-Rousan, R. Z. (2023). Impact of Internal CFRP strips on the flexural behavior of heat-damaged reinforced concrete beams. Heliyon, 9(6). doi:10.1016/j.heliyon.2023.e17145.

[9] Mohammadi-Firouz, R., Pereira, E. N. B., & Barros, J. A. O. (2023). Experimental assessment of the thermo-mechanical bond behavior of NSM CFRP with cement-based adhesives. Construction and Building Materials, 364, 129980. doi:10.1016/j.conbuildmat.2022.129980.

[10] Marid, H., & Vahidi, E. K. (2023). Experimental study on flexural behavior of reinforced lightweight concrete beams strengthening with a slurry infiltrated fiber concrete (SIFCON). Asian Journal of Civil Engineering, 1–13. doi:10.1007/s42107-023-00879-9.

[11] Carrillo, J., Ramirez, J., & Lizarazo-Marriaga, J. (2019). Modulus of elasticity and Poisson's ratio of fiber-reinforced concrete in Colombia from ultrasonic pulse velocities. Journal of Building Engineering, 23, 18–26. doi:10.1016/j.jobe.2019.01.016.

[12] Abd-Ali, M. S., & Essa, A. A. A. (2019). Mechanical properties of slurry infiltrated fibrous concrete (SIFCON) with variation steel fiber ratios and silica fume. Journal of Advanced Research in Dynamical and Control Systems, 11, 1863–1872.

[13] Servadei, F., Zoli, L., Galizia, P., Piancastelli, A., & Sciti, D. (2023). Processing and characterization of ultra-high temperature ceramic matrix composites via water based slurry impregnation and polymer infiltration and pyrolysis. Ceramics International, 49(1), 1220–1229. doi:10.1016/j.ceramint.2022.09.100.

[14] Adnan, N., Alwash, N. A., & Kadhum, M. M. (2023). Experimental Study on the Behavior of Axially Loaded Reinforced Concrete Square Columns Strengthened with SIFCON Shell. E3S Web of Conferences, 427, 2019. doi:10.1051/e3sconf/202342702019.

[15] Khamees, S. S., Kadhum, M. M., & Alwash, N. A. (2020). Experimental and numerical investigation on the axial behavior of solid and hollow SIFCON columns. SN Applied Sciences, 2(6), 1–15. doi:10.1007/s42452-020-2907-9.

[16] Tiwary, A. K., & Bhatia, S. (2020). Retrofitting techniques for reinforced and sustainable concrete column. Journal of Green Engineering, 10(9), 6858–6870.

[17] Vritesh, M. V., & Asish, S. (2021). A Comparative Analysis on the Methods of Strengthening Isolated Reinforced Concrete Columns. IOP Conference Series: Materials Science and Engineering, 1203(2), 022037. doi:10.1088/1757-899x/1203/2/022037.

[18] Suntharalingam, T., Gatheeshgar, P., Upasiri, I., Poologanathan, K., Nagaratnam, B., Rajanayagam, H., & Navaratnam, S. (2021). Numerical study of fire and energy performance of innovative light-weight 3d printed concrete wall configurations in modular building system. Sustainability (Switzerland), 13(4). doi:10.3390/su13042314.

[19] Abdulghani, A. W., & Jaafer, A. A. (2021). Comparative Numerical Study between /Steel Fiber Reinforced Concrete and SIFCON on Beam-Column Joint Behavior. Materials Science Forum, 1021, 138–149. doi:10.4028/www.scientific.net/msf.1021.138.

[20] Salehi, R., Akbarpour, A., & Shalbaftabar, A. (2020). Fire Evaluation of RC Frames Strengthened with FRPs Using Finite Element Method. American Journal of Engineering and Applied Sciences, 13(4), 610–626. doi:10.3844/ajeassp.2020.610.626.

[21] Mohammed, A. S. A., Abdullah, A. S. A., & Zayed, A. N. A. (2021). Strengthening of Reinforced Concrete Two-Way Slabs Using FRP. Reinforced Concrete Research Group, Menoufia University, Al Minufiyah, Egypt.

[22] Yoo, S. J., Yuan, T. F., Hong, S. H., & Yoon, Y. S. (2020). Effect of strengthening methods on two-way slab under low-velocity impact loading. Materials, 13(24), 1–16. doi:10.3390/ma13245603.

[23] Hashad, M., Elgendy, M., & Essam, M. Rehabilitation of reinforced concrete slabs using steel. Reinforced Concrete Research Group, Menoufia University, Al Minufiyah, Egypt.

[24] Warwar, R. S., & Said, A. I. (2021). Flexural Behavior of Reinforced Concrete Beams Covered by Gypsum Layers and Exposed to Elevated Temperatures. E3S Web of Conferences, 318, 03005. doi:10.1051/e3sconf/202131803005.

[25] Alzamili, H. H., & Elsheikh, A. M. (2023). Numerical Study of the Behavior of RC Beam At High Temperatures. Building and Reconstruction, 110(6), 58–72. doi:10.33979/2073-7416-2023-110-6-58-72.

[26] Panahi, H., & Genikomsou, A. S. (2022). Comparative Investigation of Concrete Plasticity Models for Nonlinear Finite-Element Analysis of Reinforced Concrete Specimens. Practice Periodical on Structural Design and Construction, 27(2), 4021083. doi:10.1061/(asce)sc.1943-5576.0000670.

[27] Raza, A., Khan, Q. U. Z., & Ahmad, A. (2019). Numerical investigation of load-carrying capacity of GFRP-reinforced rectangular concrete members using CDP model in Abaqus. Advances in Civil Engineering, 2019. doi:10.1155/2019/1745341.

[28] Michał, S., & Andrzej, W. (2015). Calibration of the CDP model parameters in Abaqus. Advances in Structural Engineering and Mechanics (ASEM15), 25-29 August, 2015, Incheon, Korea.

[29] Le Minh, H., Khatir, S., Abdel Wahab, M., & Cuong-Le, T. (2021). A concrete damage plasticity model for predicting the effects of compressive high-strength concrete under static and dynamic loads. Journal of Building Engineering, 44, 103239. doi:10.1016/j.jobe.2021.103239.

[30] Bakhti, R., Benahmed, B., Laib, A., & Alfach, M. T. (2022). New approach for computing damage parameters evolution in plastic damage model for concrete. Case Studies in Construction Materials, 16, 834. doi:10.1016/j.cscm.2021.e00834.

[31] Nastri, E., & Todisco, P. (2022). Macromechanical Failure Criteria: Elasticity, Plasticity and Numerical Applications for the Non-Linear Masonry Modelling. Buildings, 12(8), 1245. doi:10.3390/buildings12081245.

[32] Anas, S. M., Alam, M., & Shariq, M. (2023). Behavior of two-way RC slab with different reinforcement orientation layouts of tension steel under drop load impact. Materials Today: Proceedings, 87, 30–42. doi:10.1016/j.matpr.2022.08.509.

[33] Habeeb Albo Sabar, A., & Mansour Kadhum, M. (2022). Numerical modeling of the experimental test for shear strengthened of fire damaged high strength lightweight RC beams with SIFCON jacket. Periodicals of Engineering and Natural Sciences (PEN), 10(2), 512. doi:10.21533/pen.v10i2.2984.

[34] Cai, B., Li, B., & Fu, F. (2020). Finite Element Analysis and Calculation Method of Residual Flexural Capacity of Post-fire RC Beams. International Journal of Concrete Structures and Materials, 14(1), 58. doi:10.1186/s40069-020-00428-7.

[35] Elsheikh, A., & Alzamili, H. H. (2023). Post Fire Behavior of Structural Reinforced Concrete Member (Slab) Repairing with Various Materials. Civil Engineering Journal (Iran), 9(8), 2012–2031. doi:10.28991/CEJ-2023-09-08-013.